Scientific paper

Chromatographic Enantiomer Separation Using 9-Amino-9-(deoxy)-epiquinine-derived Chiral Selectors: Control of Chiral Recognition via Introduction of Additional Stereogenic Centers

Norbert M. Maier,* Elisa Greco, Ján Petrovaj and Wolfgang Lindner

University of Vienna, Institute of Analytical Chemistry Währingerstrasse 38, A-1090 Vienna, Austria

** Corresponding author: E-mail: norbert.maier@univie.ac.at*

Received: 16-02-2012

Dedicated to Prof. Dr. Gorazd Vesnaver on the occasion of his 70th birthday

Abstract

Three new cinchona-type chiral selectors have been prepared by attaching *N*-pivaloyl-glycine, *N*-pivaloyl-*(S)*-valine and *N*-pivaloyl-*(R)*-valine segments to the *C9*-amino function of 9-amino-9-(deoxy)-epiquinine (eAQN), and immobilized to silica to provide the corresponding chiral stationary phases (CSPs). Evaluation of the chromatographic enantioseparation characteristics of these CSPs with a broad assortment of *N*-carbamoyl protected amino acids under polar organic mobile phase conditions revealed modest chiral recognition capabilities for *N*-Fmoc-, *N*-Cbz- and *N*-Boc-derivatives. It was found that the enantioselective analyte binding to these CSPs is strictly controlled by the absolute stereochemistry of the amino acid functionalities attached to the *C9*-amino group of the eAQN framework. Specifically, the CSP derived from *(S)*-valine-based selector exhibits preferential binding of *N*-carbamoyl-*(S)*-amino acids, while the CSPs featuring *(R)*-valine- and the glycine-derived selectors show opposite enantioselective binding preference. The observed impact of analyte structure on enantioselectivity and the specific preferences in enantioselective binding point to chiral recognition mechanisms capitalizing on intermolecular ion pairing, hydrogen bonding and subtle steric interactions, with the latter making the crucial contributions to stereodiscrimination. The finding that the chiral recognition characteristics of epiquinine can be readily controlled via incorporation of additional stereogenic centers remote from the cinchona scaffold might be useful information for the design of new enantioselective receptors and organocatalysts.

Keywords: Chiral stationary phase, HPLC, enantiomer separation, epicinchona alkaloids, anion exchange, N-protected amino acids, control of enantiomer elution order

1. Introduction

Cinchona alkaloids and their derivatives have been receiving considerable attention as privileged scaffolds for the design of highly enantioselective resolving agents, auxiliaries, ligands, organocatalysts and chiral selectors (SOs). While research in the past has preferentially resorted to the readily accessible naturally occurring cinchona alkaloids,[1] recently their unnatural *C9*-epimers are finding increasing use as complementary, and often highly effective chiral scaffolds in the rapidly evolving field of enantioselective organocatalysis.[2] With respect to chiral separation applications, however, epicinchona alkaloids remain largely unexplored. Preliminary studies conducted by our group have provided evidence that derivatives of epicinchona alkaloids also may be useful as SOs for enantiomer separation applications due to chiral recognition capabilities complementary to those seen with naturally occurring cinchona alkaloids.[3–6] Nevertheless, the current lack of a sound mechanistic understanding of the factors that govern the chiral recognition processes of epi-cinchona alkaloids and their derivatives poses a serious limitation for the full exploitation of their potential.

As a continuation of our efforts, we report in this contribution on the synthesis of a new class of epicinchona-type chiral SOs, derived from 9-amino-9-(deoxy)-epiquinine (eAQN) and sterically demanding chiral and achiral amino acid motifs attached at the *C9*-position. For the establishment of qualitative structure-enantioselectivity relationships, these SOs were evaluated in immobili-

zed form with different types of *N*-carbamoyl protected amino acids (chiral analytes, SAs) under polar organic mobile phase conditions. The observed trends in enantioselectivity, retention behavior and preferences in enantioslective binding seen with these CSPs were utilized to indentify the nature of the intermolecular interactions crucial to the stereodiscrimination processes, and interpreted in terms of the underlying recognition mechanisms.

2. Experimental

2. 1. Materials

N-hydroxysuccinimide and diisopropylethylamine were from Sigma Aldrich (Vienna, Austria). Pivaloyl chloride was ordered from Fluka (Buchs, Switzerland). Glycine, *(R)*-valine, and *(S)*-valine were purchased from Bachem (Bubendorf, Switzerland). 2,2'-azo-bis-2-methylpropionitrile (AIBN) was from Merck (Darmstadt, Germany). eAQN **1** was prepared and purified following a procedure described in the literature.[7] Mercaptopropyl-modified silica (0.7 mmol thiol functions/g) was prepared starting from Prontosil 120-5 HPLC grade silica gel (5 μm, specific surface: 320 m^2/g; Bischoff Chromatography, Leonberg, Germany) following a literature procedure.[4] All solvents used for synthesis were obtained from Merck (Darmstadt, Germany) and used as received. Thin layer chromatography was performed on aluminum sheets precoated with silica 60 F254 (Merck, Darmstadt, Germany). Flash chromatographic purification of products and intermediates was carried out with Silica 60 (mean particle size 40–60 μm) from Merck (Darmstadt, Germany). *N*-Fmoc-, *N*-Cbz- and *N*-Boc-amino acids used test compounds for CSP evaluation (see Figure 1) and the corresponding enantiomers were available from previous studies, or purchased from Bachem (Bubendorf, Switzerland).

2. 2. Instrumentation

^{1}H and ^{13}C NMR spectra were acquired on an AC300 or a DRX 400 MHz spectrometer from Bruker. The chemical shifts of the protons are given in parts per million (δ ppm) with respect to tetramethylsilane as internal standard. Mass spectra were acquired with a PESciex API 365 triple quadrupole instrument (PESciex, Thornhill, Canada) using electrospray ionization. Sample solutions in appropriate solvents (chloroform or methanol)

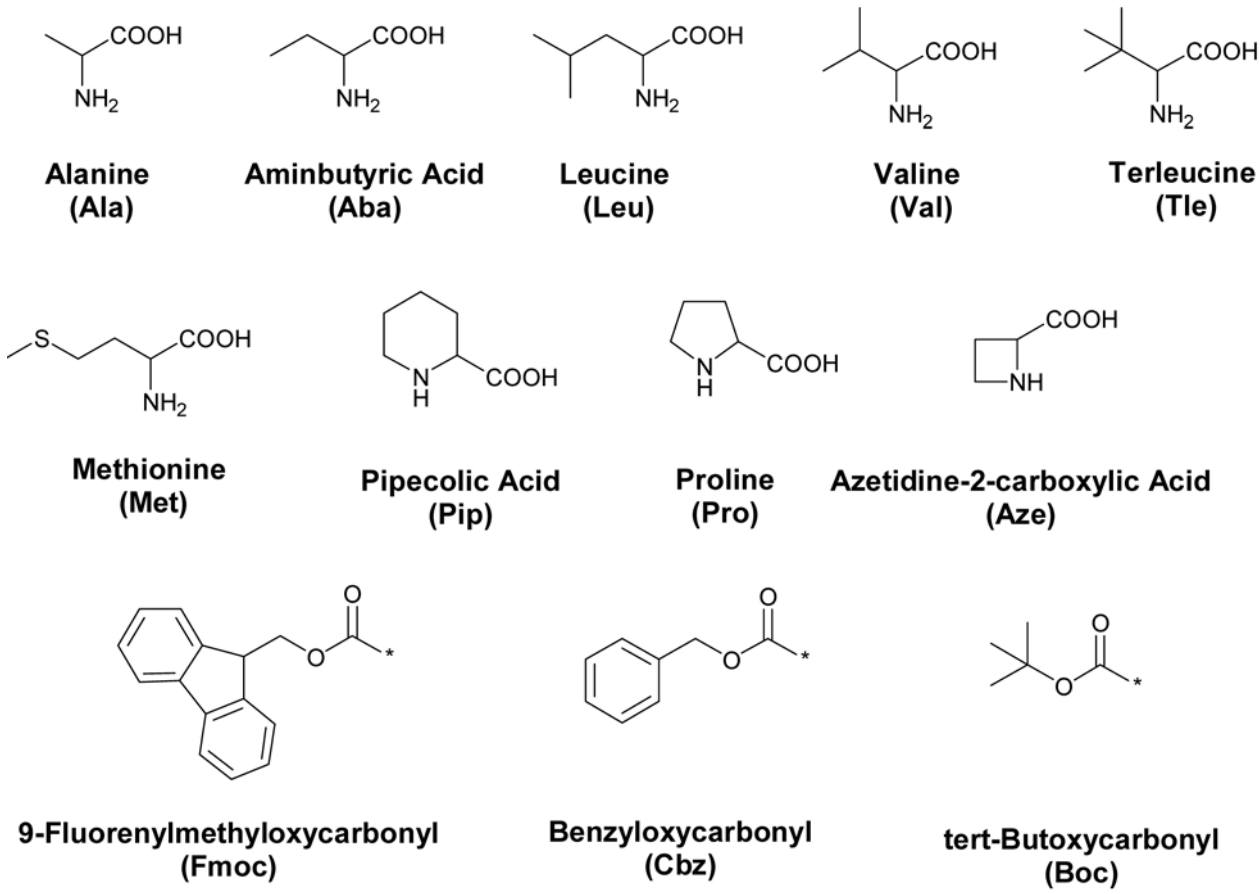

Figure 1. Chemical Structures of the investigated amino acids and the corresponding carbamoyl functions employed as *N*-protecting groups.

were infused at concentrations of approximately 0.1 mg/ml via a syringe pump (Harvard Apparatus, SO Natick, USA) at a flow rate of 5 μL/min. The electrospray voltage was typically set to 5250 V. Infrared spectra were measured on a Bruker Model Tensor 27 FTIR spectrometer equipped with an ATR unit, employing the samples either as solids, or as films coated from saturated dichlormethane solutions. Optical rotation values were recorded with a Perkin-Elmer 341 polarimeter at 25 °C. The chemical purity of compounds **4a-c** was established by gradient RP-HPLC, using the following conditions: Column: Agilent XDB-C18, 150 × 4.6 μm i.d., 5 mm; Mobile phase A: water-acetonitrile-diethylamine-trifluoroacetic acid 90:10:0.2:0.1 (v/v), Mobile Phase B: acetonitrile-diethylamine-trifluoroacetic acid 100:0.2:0.1; Gradient: 0.0–5.0 min: 100% A; 5.0–15.0 min: 95% B, 15.0–20.0 min: 95% B; 20.01–25.0 min: 100% A; flow rate: 1.0 mL/min. UV detection at 280 nm, reference wavelenght 360 nm; column temperature: 30 °C. Samples concentration: 5.0 mg/μL; injected sample volume: 2.0 mL.

2. 3. Synthesis

2. 3. 1. 2,5-Dioxopyrrolidin-1-yl pivalate[8] (3)

N-hydroxysuccinimide (4.68 g, 40.7 mmol) and diisopropylethylamine (5.25 g, 40.7 mmol) were dissolved in 50 mL of dry THF. To the stirred solution, pivaloyl chloride (4.70 g; 38.7 mmol) in 20 mL of dry THF was added drop wise at ambient temperature. Stirring was continued for 3 h. The precipitated amine hydrochloride was removed by filtration and washed with a small portion of dry THF. The combined filtrates were concentrated under reduced pressure to give a white solid. This was taken into 100 ml ethyl acetate, washed with 2 M aqueous HCl (50 ml), 5% aqueous $NaHCO_3$, and with water (2 × 50 mL). The organic layer was dried ($MgSO_4$) and evaporated to yield a yellowish solid. The crude product was purified by crystallization from ethyl acetate:hexane (3:1 (v/v)). Yield after drying at 40 °C in vacuum: 5.09 g colorless leaflets (25.5 mmol, 66%). M.p.: 75–77 °C; Lit.: m.p.: 77–78 °C[8]; ^{1}H NMR ($CDCl_3$) δ: 2.80 (4H, s, broad) and 1.39 ppm (9H, s).

2. 3. 2. N-pivaloyl Amino Acids[9-12] (2a-c)

The following general procedure was used for the preparation of the *N*-pivaloyl derivatives **2a**-**c** of glycine, *(R)*-valine, and *(S)*-valine: The corresponding amino acid (20 mmol) and $NaHCO_3$ (3.4 g, 40.4 mmol) were dissolved in 100 mL water. To the clear solution, succinimide ester **3** (2.8 g; 14 mmol) was added and the heterogeneous mixture was stirred for 4 h at ambient temperature. Unconsumed active ester was removed by filtration and the filtrate was acidified with concentrated aqueous HCl to pH 2.0. The acidic solution was saturated with sodium chloride and extracted with ethyl acetate (3 × 50 mL). The combined organic phases were dried ($MgSO_4$) and concentrated under reduced pressure to give a solid. The crude product was recrystallized from ethyl acetate and petroleum ether and dried in high vacuum at 40 °C. Compound **2a**: yield 1.98 g (12.44 mmol, 88%), m.p. 134–135 °C, Lit.: m.p. 131–133 °C[9]; ^{1}H NMR (400 MHz, CD_3OD) δ: 4.85 (2H, s, broad), 1.19 ppm (9H, s); ATR-FTIR (solid): 3403, 2965, 1740, 1609, 1528, 1482 cm^{-1}; MS *m/z* (M-H$^+$): calculated for $C_7H_{13}NO_3$: 160.1, found: 160.3; Compound **2b**: yield 2.01 g (9.98 mmol, 71%), m.p. 138–140 °C, ^{1}H NMR (400 MHz, $CDCl_3$) δ: 9.95 (1H, s, broad), 6.26 (1H, d, broad, J = 8.52 Hz), 4.63 (1H, dd, J_1 = 8.45 Hz, J_2 = 4.56 Hz), 2.22 (1H, m), 1.21 (9H, s), 0.97 (6H, overlapped d's, J = 6.8 Hz); ATR-IR (solid): 3434, 2968, 1724, 1631, 1519, 1468 cm^{-1}; MS *m/z* (M-H$^+$): calculated for $C_{10}H_{19}NO_3$: 202.1, found: 202.2; $[\alpha]_{436}$ = +35.7; $[\alpha]_{546}$ = +18.3, $[\alpha]_{589}$ = +15.0, (c = 1.0, ethyl acetate); Lit.: $[\alpha]_{589}$ = –20.1, (c = 0.49, chloroform)[10]. Compound **2c**: yield 1.98 g (9.84 mmol, 70%), m.p. 138–140 °C, ^{1}H NMR (400 MHz, $CDCl_3$) δ: 9.95 (1H, s, broad), 6.26 (1H, d, broad, J = 8.52 Hz), 4.63 (1H, dd, J_1 = 8.45 Hz, J_2 = 4.56 Hz), 2.22 (1H, m), 1.21 (9H, s), 0.97 (6H, overlapped d's, J = 6.8 Hz); ATR-FTIR (solid): 3435, 2968, 1727, 1633, 1519, 1468 cm^{-1}; MS *m/z* (M-H$^+$): calculated for $C_{10}H_{19}NO_3$: 202.1, found: 202.2; $[\alpha]_{436}$ = –35.3; $[\alpha]_{546}$ = –18.5, $[\alpha]_{589}$ = –15.3, (c = 1.0, ethyl acetate).

2. 3. 3. Selectors (4a-c)

The corresponding *N*-pivaloyl-amino acid (5.0 mmol) and diisopropylcarbodiimide (0.63 g; 5.0 mmol) were dissolved in 20 mL of dry THF. The mixture was stirred for 30 min at 25 °C. A white precipitate was formed within minutes after addition, indicating the generation of the corresponding anhydride. A solution of amine **1** (0.81 g, 2.5 mmol) in 7 mL dry THF was added drop wise and the reaction mixture was allowed to react at ambient temperature. The progress of the reaction was monitored by TLC analysis (silica, $CHCl_3$: MeOH = 5:1, (v/v)). After complete consumption of the amino acid derivatives, the solvent was evaporated under reduced pressure. The residue was treated with a mixture of hexane:ethyl acetate (3:1, v/v, 20 mL) and the insoluble urea was removed by filtration. The urea was washed with another 20 ml hexane:ethyl acetate (3:1, (v/v)). The combined filtrates were concentrated under reduced pressure to give the crude products as yellow oils. These were purified by chromatography (silica, mobile phase: first $CHCl_3$, then $CHCl_3$: MeOH 10:1 (v:v)). Evaporation of the pooled pure fractions yielded the products as colorless foams.

Compound **4a** (Gly-eAQN): 780 mg, (1.68 mmol, 67%); ^{1}H NMR (400 MHz, $CDCl_3$) δ : 8.73 (1H, d, J = 4.6 Hz), 8.03 (1H, d, J = 9.2 Hz), 7.78 (1H, s, broad), 7.60 (1H, s), 7.40 (1H, dd, J_1 = 9.2 Hz, J_2 = 2.7 Hz), 7.32 (1H, d, J = 4.6 Hz); 6.48 (1H, t, broad), 5.72 (1H, m), 5.43 (1H,

s, very broad), 5.01 (2H, m), 4.00 (1H, dd, J_1 = 16.5 Hz, J_2 = 5.4 Hz), and 3.81 (1H, dd, J_1 = 16.6 Hz, J_2 = 4.6 Hz), 3.98 (3H, s), 3.31–3.17 (3H, overlapping m´s), 2.88–2.73 (2H, overlapping m´s), 2.37 (m, 1H), 1.75 (1H, m), 1.70 (1H, m), 1.52 (1H, m), 1.12 (9H, s) and 1.02–0.91 ppm (2H, overlapping m´s); ^{13}C NMR (100 MHz, $CDCl_3$) δ: 179.1, 169.4, 158.3, 147.9, 145.2, 141.4, 132.3, 122.0, 115.1, 102.1, 58.7, 56.3, 56.0, 43.5, 41.4, 39.8, 39.0, 28.2, 27.8, 27.7, 26.5, 18.9 ppm; ATR-FTIR (neat film): 3308, 2934, 1643, 1622, 1590, 1507, 1475, 1364, 1263, 1228 cm^{-1}; HR MS *m/z* (M-H$^+$): calculated for $C_{27}H_{36}N_4O_3$: 465.2787, found: 465.2862; $[\alpha]_{436}$ = –7.0; $[\alpha]_{546}$ = +2.3, $[\alpha]_{589}$ = +2.9, (c = 10.0, methanol). Gradient RP chromatography: elution time 13.1 min, chemical purity > 98% by area at 280 nm.

Compound **4b** (*(S)*-Val-eAQN): 730 mg, (1.44 mmol, 49%). ^{1}H NMR (400 MHz, $CDCl_3$) δ : 8.70 (1H, d, J = 4.5 Hz), 8.01 (1H, d, J = 9.3 Hz), 7.78 (1H, s, broad),

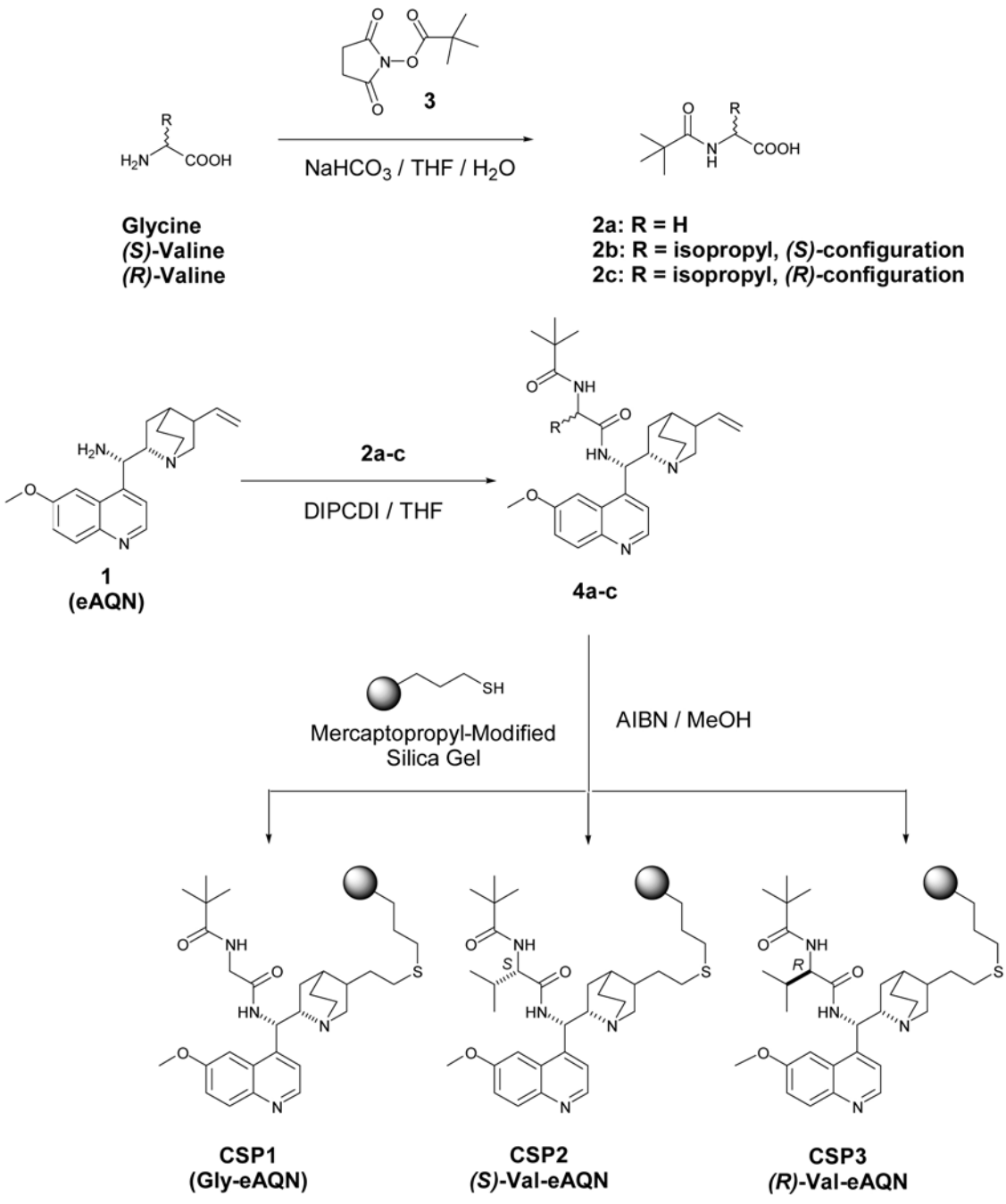

Scheme 1. Synthesis strategy employed for the preparation of CSPs 1-3

7.60 (1H, s, broad), 7.38 (1H, dd, J_1 = 9.3 Hz, J_2 = 2.6 Hz), 7.25 (1H, J = 4.2 Hz); 6.00 (1H, broad), 5.70 (1H, m), 5.35 (1H, s, very broad), 4.95 (2H, m), 4.20 (1H, dd, J_1 8.8 Hz, J_2 = 7.2 Hz), 3.98 (3H, s), 3.21 (1H, dd), 3.05 (1H, s, broad), 2.80–2.63 (2H, overlapping m´s), 2.51 (1H, s, broad), 2.30 (1H, m), 2.05 (1H, m), 1.69 (1H, m) and 1.60 ppm (2H, overlapping m´s), 1.45 (1H, m), 1.08 (9H, s), 1.00 (1H, m), 0.94 (3H, d, J = 6.8 Hz) and 0.89 ppm (3H, d, 6.8 Hz); ^{13}C NMR (100 MHz, $CDCl_3$) δ: 179.2, 147.9, 141.6, 132.3, 121.9, 115.0, 58.5, 56.3, 55.9, 41.3, 39.9, 39.2, 31.3, 28.4, 27.8, 27.7, 19.6, 18.5 ppm. ATR-FTIR (neat film): 3320, 2958, 1639, 1590, 1506, 1474, 1365, 1263, 1227 cm^{-1} HR MS *m/z* (M-H$^+$): calculated for $C_{30}H_{42}N_4O_3$: 507.3335; found: 507.3335; $[\alpha]_{436}$ = –117.0; $[\alpha]_{546}$ = –52.6, $[\alpha]_{589}$ = –41.8, (c = 10.0, methanol). Gradient RP chromatography: elution time 14.5 min, chemical purity > 98% by area at 280 nm.

Compound **4c** (*(R)*-Val-eAQN): 960 mg, (1.90 mmol, 76%) ; ^{1}H NMR (400 MHz, $CDCl_3$) δ : 8.72 (1H, d, J = 4.7 Hz), 8.03 (1H, d, J = 9.2 Hz), 7.40 (1H, s, broad), 7.39 (1H, dd, J_1 = 9.4 Hz, J_2 = 2.5 Hz), 7.32 (1H, d, J = 3 Hz), 6.25 (1H, d, broad); 5.69 (1H, m), 5.35 (1H, s, broad), 4.96 (2H, dd), 4.40 (1H, dd, J_1 = 8.8 Hz, J_2 = 5.5 Hz), 3.98 (3H, s), 3.27 (1H, dd), 3.05 (1H, s, broad), 2.80–2.63 (2H, overlapping m´s), 2.41 (1H, s, broad), 2.30 (1H, m), 2.05 (1H, m), 1.69(1H, m), 1.60 (2H, overlapping m´s), 1.54 (1H, m), 1.20 (9H, s), 1.00 (1H, m), 0.94 (1H, m), 0.80 (3H, d, J = 6.9 Hz) and 0.72 ppm (3H, broad); ^{13}C NMR (100 MHz, $CDCl_3$) δ: 178.8, 147.9, 141.6, 132.3, 115.0, 57.6, 56.3, 56.0, 41.3, 39.9, 39.3, 32.4, 28.3, 27.9, 27.7, 19.7 ppm. ATR-FTIR (neat film): 3309, 2959, 2869, 1637, 1590, 1507, 1475, 1433, 1364, 1262, 1227 cm^{-1}; HR MS *m/z* (M-H$^+$): calculated for $C_{30}H_{42}N_4O_3$: 507.3335; found: 507.3330; $[\alpha]_{436}$ = –140.2; $[\alpha]_{546}$ = +18.5, $[\alpha]_{589}$ = +30.0, (c = 10.0, methanol). Gradient RP chromatography: elution time 15.1 min, chemical purity > 98% by area at 280 nm.

2. 3. 4. CSPs 1-3

Selectors **4a**, **4b**, and **4c** (1.18 mmol) were dissolved in methanol (10 mL) and transferred into a 250 mL-reactor equipped with a mechanical stirrer, an oil bath, a reflux condenser and a nitrogen line. Mercaptopropyl silica (3.0 g) and AIBN (9.68 mg; 5.0 mol-% selector, 0.059 mmol) were added and the mixture was stirred for 10 min. The resultant suspension was refluxed under nitrogen atmosphere for 7 hours with gentle mechanical stirring. The modified silicas were isolated by filtration through a sintered-glass funnel (porosity 4) and washed with methanol (5 × 60 mL), 5% acetic acid in methanol (2 × 60 mL), and methanol (2 × 60 mL). The materials were dried at 60°C. **CSP1** (Gly-eAQN) CHN analysis: 11.85% C, 1.76% H, 1.37% N; loading level based on N: 244 μmol/g; **CSP2** (*(S)*-Val-eAQN) CHN analysis: 13.70% C, 2.01% H, 1.49% N; loading level based on N: 266 μmol/g; **CSP3** (*(R)*-Val-eAQN) CHN analysis: 13.02% C, 1.93% H, 1.41% N; loading level based on N: 251 μmol/g.

2. 4. Chromatography

2. 4. 1. Instrumentation

High pressure liquid chromatographic measurements were performed with a HP 1050 HPLC system, consisting of a four-channel gradient pump, a variable wavelength detector and an autosampler. Data were recorded and processed using HP ChemStation Software.

2. 4. 2. CSPs

CSPs 1-3 were packed into stainless steel columns (150 × 4 mm I.D.) employing a standard slurry packing procedure (Bischoff Chromatography, Leonberg, Germany). Prior to use, the columns were equilibrated with 2-propanol (30 min, 0.5 mL/min), methanol (30 min, 1 mL/min) and finally mobile phase (60 min, 1 mL/min).

2. 4. 3. Chromatographic Conditions

All chromatographic measurements were performed employing 1.0% acetic acid in methanol (v/v) as mobile phase. The flow rate was 1.0 mL/min. Signals were detected at 230 nm (*N*-Boc-amino acids) and 254 nm (*N*-Cbz- and *N*-Fmoc-amino acids), respectively. The column temperature was kept constant at 25±0.1 °C by means of a column oven.

3. Results and Discussion

3. 1. Synthetic Aspects

The SOs **4a**-**c** were prepared from the corresponding N-pivaloyl amino acids **2a-c** and eAQN **1** following the route outlined in **Scheme 1**. The strategy involved the preparation of **1** from quinine following a literature procedure, using a Mitsunobu-type reaction employing an azide nucleophile and subsequent Staudinger reduction.[7] *N*-pivaloyl derivatives **2a**-**c** were prepared from glycine, and *(S)*- and *(R)*-valine via a mild acylation protocol employing 2,5-dioxopyrrolidin-1-yl pivalate **3** in presence of aqueous sodium bicarbonate. Coupling of the amino acid intermediates **2a**-**c** with **1** was accomplished via activation with diisopropylcarbodiimide in anhydrous THF. The observed reaction rates were rather slow (complete coupling required 5–30 h at ambient temperature). After chromatographic purification, SOs **4a**-**c** were obtained in yields ranging from 49% to 76%. SOs **4a**-**c** were covalently immobilized to mercaptopropyl-modified silica gel to obtain the corresponding **CSPs 1-3**. The required mercaptopropyl-modified silica gel was prepared by a base-catalyzed condensation of mercaptopropyl trimethoxysi-

lane to HPLC-grade spherical particles following a literature procedure.[4] SO immobilization was performed under free radical addition conditions, establishing a robust covalent thioether linkage between the solid-phase supported thiol groups and the terminal olefin function implemented in the quinuclidine unit of SOs **4a-c**. All immobilization experiments were carried out at constant thiol/selector mol-ratios to realize similar ligand surface loading levels for **CSPs 1-3**. Immobilization procedures carried out under these carefully controlled conditions indeed provided CSPs with fairly consistent levels of SO loading (0.24–0.27 mmol SO units/g of modified silica gel).

3. 2. Chromatographic Evaluation of CSPs 1-3

The chromatographic evaluation of **CSPs 1-3** was carried out under identical experimental conditions to establish a body of data suitable for extracting valid information on the underlying chiral recognition phenomena occurring between the tested SAs and the immobilized SOs. It is important to realize that retention and relative retention data provide valid approximations for the inherent binding affinity and enantioselectivity only under conditions that render nonspecific contributions to overall SA retention negligible.[13] Previous studies have provided compelling evidence that this crucial requirement is met with cinchona alkaloid-based CSPs operated in polar organic mobile phases,[14] i.e. under the chromatographic conditions employed in this study. Consequently, in the following the acquired body of chromatographic data is directly employed for the comparative thermodynamic interpretation of chiral recognition characteristics. With the focus of the present study being on mechanistic rather than application-oriented aspects, only thermodynamic relevant chromatographic performance parameters (i.e., retention factors, enantioselectivity factors, and elution orders) are reported. However, it is worth noting that the investigated columns, packed with **CSPs 1-3,** displayed quite favorable kinetic performance characteristics. Thus, the observed column efficiencies were in the range of 30,000 to 45,000 plates/meter. Given their relatively high performance, these columns are capable of producing sufficiently high levels of chromatographic resolution to allow baseline separations for SAs exhibiting enantioselectivity factors of $\alpha > 1.1$. Representative chromatograms for *N*-Cbz-leucine are shown in Figure 2.

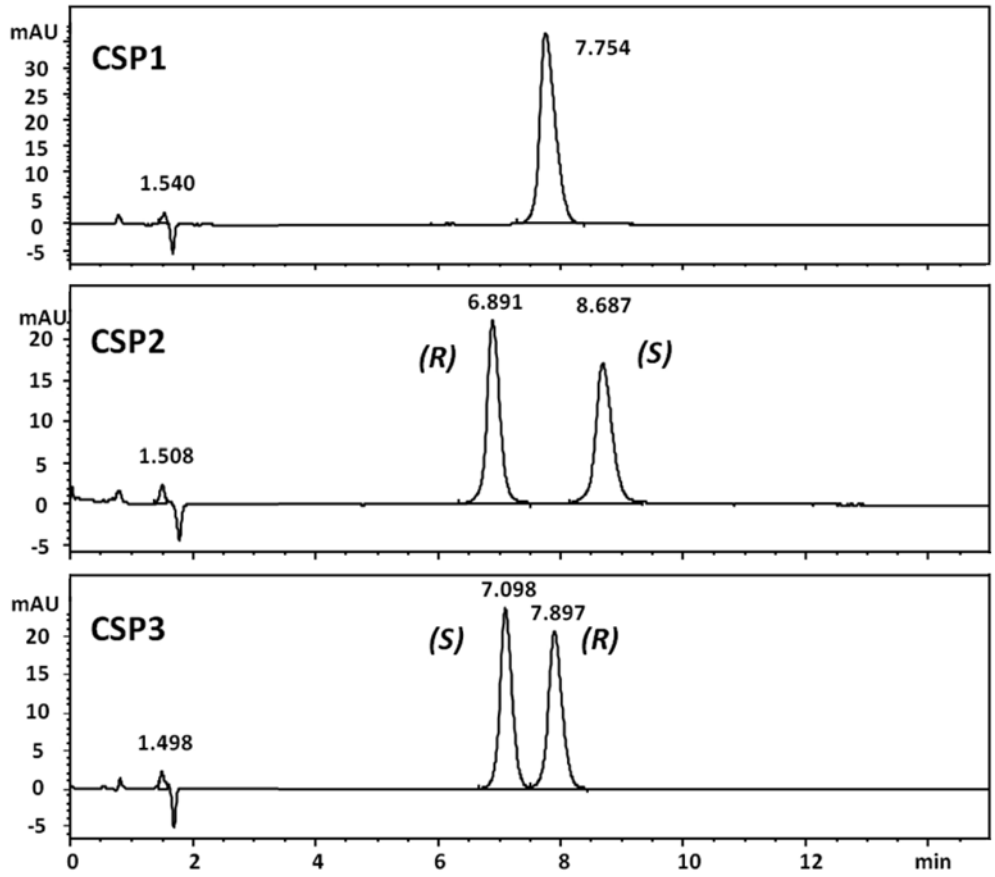

Figure 2. Chiral recognition behavior of *N*-Cbz-leucine on **CSPs 1-3** using polar organic mobile phase conditions. Chromatogram obtained with A) the Gly-eAQN-, B) (S)-Val-eAQN- and C) (R)-Val-eAQN-derived CSP, respectively. Note the reversal of enantiomer elution order occurring upon changing from CSP2 to CSP3. For chromatographic conditions see Table 2.

Table 1. Chromatographic enantiomer separation data for *N*-Fmoc amino acids obtained on CSPs 1-3

	CSP1 Gly-eAQN			CSP2 *(S)*-Val-eAQN			CSP3 *(R)*-Val-eAQN		
Fmoc AA	**k_2**	**α**	**e.o.**	**k_2**	**α**	**e.o.**	**k_2**	**α**	**e.o.**
Ala	12.57	1.05	R	11.35	1.21	S	14.08	1.16	R
Aba	10.54	1.06	R	9.09	1.17	S	11.88	1.16	R
Met	18.99	1.04	R	18.45	1.31	S	22.86	1.18	R
Leu	8.06	1.06	R	8.47	1.39	S	9.32	1.23	R
Val	8.25	1.08	R	6.36	1.05	S	9.43	1.19	R
Tle	5.67	1.11	R	4.72	1.15	S	6.49	1.15	R
Aze	35.81	1.13	R	22.53	1.15	R	34.01	1.17	R
Pro	17.73	1.08	R	11.76	1.11	R	16.12	1.19	R
Pipe	9.27	1.08	R	6.56	1.07	n.d.	10.49	1.29	R

Chromatographic conditions: Columns (150 × 4.6 mm i.d.); mobile phase: acetic acid (1.0% v/v) in methanol; flow rate: 1.0 mL/min; UV-detection: 254 or 230 nm; k_2: retention factor of the more strongly retained enantiomer; α: enantioselectivity; e.o.: elution order indicating the more strongly retained enantiomer; n.d.: no data available.

Table 2. Chromatographic enantiomer separation data for *N*-Cbz amino acids obtained on CSPs 1-3

	CSP1 Gly-eAQN			CSP2 *(S)*-Val-eAQN			CSP3 *(R)*-Val-eAQN		
Fmoc AA	**k_2**	**α**	**e.o.**	**k_2**	**α**	**e.o.**	**k_2**	**α**	**e.o.**
Ala	7.31	1	n.d.	6.87	1.22	S	7.6	1.12	R
Aba	6.18	1	n.d.	5.6	1.18	S	6.54	1.13	R
Met	11.55	1	n.d.	11.41	1.28	S	12.79	1.15	R
Leu	4.82	1	n.d.	5.14	1.37	S	5.07	1.16	R
Val	n.d.	n.d.	n.d.	n.d.	n.d.	n.d.	n.d.	n.d.	n.d.
Tle	3.48	1.04	R	2.97	1.1	S	3.73	1.15	R
Aze	18.38	1.15	R	12.62	1.17	R	14.72	1.11	R
Pro	9.78	1.05	R	6.07	1	n.d.	7.47	1	R
Pipe	5.23	1.06	R	3.9	1	n.d.	4.75	1.12	R

Chromatographic conditions: Columns (150 × 4.6 mm i.d.); mobile phase: acetic acid (1.0% v/v) in methanol; flow rate: 1.0 mL/min; UV-detection: 254 or 230 nm; k_2: retention factor of the more strongly retained enantiomer; α: enantioselectivity; e.o.: elution order indicating the more strongly retained enantiomer; n.d.: no data available.

Table 3. Chromatographic enantiomer separation data for *N*-Boc amino acids obtained on CSPs 1-3

	CSP1 Gly-eAQN			CSP2 *(S)*-Val-eAQN			CSP3 *(R)*-Val-eAQN		
Fmoc AA	**k_2**	**α**	**e.o.**	**k_2**	**α**	**e.o.**	**k_2**	**α**	**e.o.**
Ala	3.33	1	n.d.	2.73	1.28	S	2.96	1.1	R
Aba	2.91	1	n.d.	2.26	1.23	S	2.58	1.09	R
Met	5.36	1	n.d.	4.57	1.31	S	5.03	1.11	R
Leu	2	1	n.d.	2.05	1.42	S	2.01	1.1	R
Val	2.45	1	n.d.	1.76	1.12	S	2.21	1.12	R
Tle	1.72	1	n.d.	1.22	1.09	S	1.51	1.08	R
Aze	6.61	1.06	R	3.01	1	n.d.	4.28	1	n.d.
Pro	2.75	1	n.d.	1.3	1	n.d.	1.79	1	n.d.
Pipe	1.58	1	n.d.	1.07	1.05	S	1.44	1.05	R

Chromatographic conditions: Columns (150 × 4.6 mm i.d.); mobile phase: acetic acid (1.0% v/v) in methanol; flow rate: 1.0 mL/min; UV-detection: 254 or 230 nm; k_2: retention factor of the more strongly retained enantiomer; α: enantioselectivity; e.o.: elution order indicating the more strongly retained enantiomer; n.d.: no data available.

3. 3. Chromatographic Performance Characteristics of CSPs 1-3

The retention data of **CSPs 1-3** summarized in Table 1-3 demonstrate that the immobilized eAQN-type SOs exhibit considerable binding affinities for the tested SAs under the employed mobile phase conditions. The pronounced retention behavior is characteristic of the involvement of strong electrostatic interactions as the dominating intermolecular binding increment. The retention is also influenced by the nature of the *N*-protecting group present in the SAs, with the binding affinities for compounds bearing aromatic motifs (*N*-Fmoc and *N*-Cbz) being significantly higher than those seen for the corresponding *N*-Boc derivatives. This observation reflects the significant contributions of intermolecular π-π-interactions operating between the aromatic structure elements of *N*-Fmoc and *N*-Cbz derivatives and the quinoline group of the eAQN scaffold. Little difference, however, is seen when comparing the retention behaviors of given *N*-carbamoyl amino acids on the different CSPs. Evidently, all CSPs are capable of establishing the same types of high affinity interactions with the SAs under investigation.

The enantioselectivity data reported in **Tables 1-3** show that **CSPs 1-3** exhibit relatively modest levels of enantioselectivity for the tested classes of SAs. The observed enantioseparation factors range from α = 1.05–1.42, corresponding to rather small differential free energies of binding ($\Delta\Delta G$ = 130–870 J/mol). As a general trend, the *(S)*-Val-eAQN SO incorporated in **CSP2** shows overall higher levels of enantioselectivity as compared to **CSP3**, featuring the *(R)*-Val-eAQN SO system. The enantioseparation capabilities of the **CSP1** are poor, with the embedded Gly-eAQN SO failing to resolve a considerable number of the tested *N*-Cbz- and *N*-Boc-amino acid derivatives. Some trends in enantioselectivity as a function of structural features of the amino acids are seen with **CSPs 1-3.** Specifically, in the case of *N*-Fmoc derivatives, amino acids exhibiting long and flexible side chains (Met, Leu) are better resolved than those with branched (Val, Tle) or cyclic motifs, a behavior that is particularly evident with **CSP2.** Interestingly, **CSP3** exhibits superior chiral discrimination potential for the *N*-Fmoc derivatives of cyclic amino acids (Aze, Pro, Pipe) relative as compared to **CSP1** and **CSP2.**

3. 4. Preferential Enantiomer Binding of CSP 1-3

The enantiomer elution orders reported in **Table 1-3** demonstrate that the SOs incorporated in **CSP2** and **CSP3** exhibit opposite enantioselective binding preferences essentially for the entire set of evaluated *N*-carbamoyl amino acids, except for the cyclic derivatives lacking an amide-type hydrogen donor motif. Specifically, **CSP3** binds preferentially the *(R)*-enantiomers, while **CSP2** shows an opposite chiral recognition preference. The elution order trend seen with **CSP1** parallels that of **CSP3**, for the rather limited number of analytes that could be resolved. Chromatograms obtained on **CSPs 1-3** demonstrating the observed chiral recognition preferences for *N*-Cbz-leucine are shown in Figure 2. This important finding suggests that the chiral recognition preferences of the investigated SOs are controlled by the remote "attached chirality" provided by the valine segments rather than by the "built-in" stereogenic features of the eAQN component. In this context, it is worth noting that this particular mode of enantioselective binding deviates from that observed with the well-established quinine and quinidine carbamate-type SOs, for which enantiomer elution orders for *N*-acylated amino acids are strictly controlled by the *C8/C9*-stereochemistry of the parent cinchonan scaffolds[3].

3. 5. Mechanistic Considerations

On the basis of the combined chromatographic findings outlined in the preceding sections, some general conclusions can be drawn concerning the role of the SA structures on chiral recognition event. Since a negligible impact of the nature of *N*-protecting groups attached to the SAs on the enantioselectivity was observed, it is justified to assume that these functionalities are not crucially involved in the chiral recognition processes. The fact that side chain

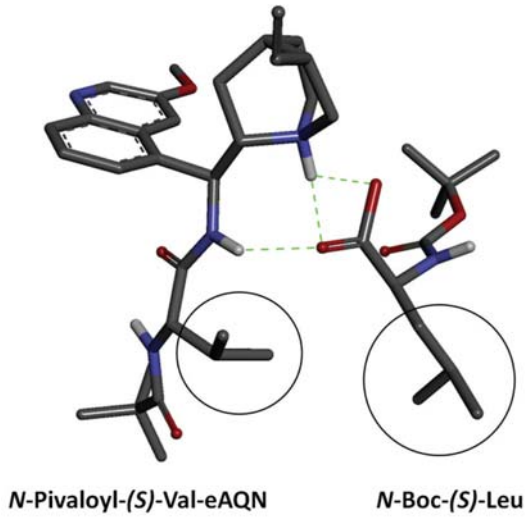

Figure 3. Tentative chiral recognition mode of selector **4b** and the more strongly interacting ***N*-Boc-*(S)*-leucine** enantiomer. The depicted selector-analyte complex is stabilized by strong electrostatic ionpairing and hydrogen bonding interactions (indicated by the green lines) occurring between the de-protonated carboxylic group of the analyte, and the protonated quinuclidine nitrogen center and the *C9*-amide group of the selector, respectively. Stereodiscrimination between the individual enantiomers emerges from favorable/unfavorable steric interactions between the sterically demanding alkyl groups (structure elements highlighted by the black circles) integrated in selector and analyte. The depicted molecular model was generated using Discovery Studio 3.1 Visualizer Software (Accelrys).

motifs of the investigated SAs do have a significant influence on the enantioselectivity suggests that these structural features play key roles in the stereodiscrimination event.

Merging the experimentally established information on the chiral recognition characteristics of **CSP1-3** with well-founded knowledge on the preferred low-energy conformations of amide derivatives of eAQN amide derivatives[15] allows proposing a tentative mechanistic picture of SO-SA interactions involved in enantioselective binding.

The essential features of this interaction mode are exemplified for the more stable diastereomeric complex between the *(S)*-valine-derived SO **4b** and *N*-Boc-*(S)*-Leu in **Figure 3**. Herein, the eAQN-derived SO is represented in the energetically favorable *open* conformation, in which the protonated quinuclidine nitrogen points away from the quinoline plane. The amino acid segment attached to the *C9*-position is aligned in an extended fashion, forming a rather shallow L-shaped binding domain with the quinuclidine group. The preferentially bonded *N*-Boc-*(S)*-Leu SA is docked into this binding site so as to permit the formation of multiple hydrogen bonds between the deprotonated carboxylic group of the SA and the quinuclidine nitrogen and *C9*-NH group. The side chain of the SA is aligned parallel to the *(S)*-valine segment, thus avoiding steric collision with the isopropyl function of the SO. The *N*-Boc group is located in a remote position from the SO, consistent with the lack of stereoselective interactions emerging from this substructure element. This proposed model rationalizes chiral discrimination on the basis of ion pairing and hydrogen bonding of the carboxylic function with the quinuclidine nitrogen and the *C9*-NH, and simultaneously occurring steric interaction between the side chains of the SO- and SA-located amino acid motifs. Note that utilizing an analogous docking mode for the corresponding *(R)*-enantiomer of the amino acid derivative would result in steric clashes between these side chains, and therefore complex destabilization. Using the proposed model, also the opposite enantioselective binding preference observed with SO **4c** for *N*-Boc-Leu enantiomers can be understood as a consequence of the mutually inverted arrangement of the critical sterically discriminating structure elements encountered in this SO-SA combination. The proposed interaction mode also rationalizes the relatively poor enantioselectivity seen with the glycine-derived SO **4a**. Obviously, with this SO the spatial demands emerging from the *C9*-segment are significantly diminished so as to permit access to both enantiomers, even of bulky SAs, with little steric discrimination.

It is important to appreciate that the macroscopic observable chromatographic elution order reflects the relative contributions of all energy-allowed diastereomeric SO-SA complexes formed between interacting species rather than that of a single or a few energetically favorable associates. Although in reasonable agreement with the entire body of experimental data, the currently still tentative nature of the proposed model needs to be emphasized. Certainly, further investigations involving more sophisticated methodologies capable of molecular-level resolution of structural details (e.g., NMR, X-ray structure analysis) will be required to substantiate the proposed model. Nevertheless, the outlined mechanistic picture still may have the potential to provide some guidance and inspiration for the development of new eAQN-based chiral selector systems and possibly organocatalysts.

4. Conclusions

Three new cinchona-type chiral selectors have been prepared by attaching *N*-pivaloyl-glycine, *N*-pivaloyl-*(S)*-valine and *N*-pivaloyl-*(R)*-valine segments to the *C9*-amino function of 9-amino-9-(deoxy)-epiquinine (eAQN), and immobilized to silica to provide the corresponding chiral stationary phases (CSPs). Evaluation of the chromatographic enantioseparation characteristics of these CSPs with a broad assortment of *N*-carbamoyl protected amino acids under polar organic mobile phase conditions revealed modest chiral recognition capabilities for *N*-Fmoc-, *N*-Cbz and *N*-Boc-derivatives. It was found that the enantioselective binding of this class of SAs to these CSPs is controlled by the absolute stereochemistry of the amino acid functionalities attached to the *C9*-amino group of the eAQN framework.

The combined experimental evidence emerging from this study is consistent with an intermolecular recognition mechanisms capitalizing on intermolecular ion pairing, hydrogen bonding, and steric interactions, with the latter evidently making the crucial contributions to stereodiscrimination. The finding that the chiral recognition characteristics of epi-cinchona alkaloids can be readily modified, amplified and even re-programmed via incorporation of additional stereogenic centers remote from the cinchona scaffold might be useful information for workers concerned with the development of new enantioselective receptors and catalysts.

5. References

1. K. Kacprzak, J. Gawroski, *Synthesis* **2001**, 961–998.
2. S. H. McCooey, S. J. Connon, *Angew. Chem. Int. Ed.* **2005**, *44*, 6367–6370; E. M. O. Yeboah, S. O. Yeboah, G. S. Singh, *Tetrahedron* **2011**, *67*, 1725–1762; B. Vakulya, S. Varga, T. Soós, *J. Org. Chem.* **2008**, *73*, 3475–3480; C. Liu, Q. Zhu, K.-W. Huang, Y. Lu, *Org. Lett.* **2011** *13*, 2638–2641; P. Kwiatkowski, T. D. Beeson, J. C. Conrad, D. W. C. MacMillan, *J. Am. Chem. Soc.* **2011**, *133*, 1738–1741; S. E. Park, E. H. Nam, H. B. Jang, J. S. Oh, S. Some, Y. S. Lee, C. E. Song, *Adv. Synth. Catal.* **2010**, *352*, 2211–2217; P. Li, S. H. Chan, A. S. C. Chan, F. Y. Kwonga, *Adv. Synth. Catal.* **2011**, *353*, 1179–1184; C. G. Oliva, A. M. S. Silva, D. I. S. P. Resende, F. A. A. Paz, J. A. S. Cavaleiro, *Eur. J. Org. Chem.* **2010**, 3449–3458.

3. N. M. Maier, L Nicoletti, M. Lämmerhofer, W. Lindner, *Chirality* **1999**, *11*, 1999, 522–528.
4. C. Czerwenka, M. Lämmerhofer, N. M. Maier, K. Rissanen, W. Lindner, *Anal. Chem.* **2002**, *74*, 5658–5666.
5. K. H. Krawinkler, N. M. Maier, R. Ungaro, F. Sansone, A. Casnati, W. Lindner, *Chirality* **2003**, *15*, S17–S29.
6. K. H. Krawinkler, N. M. Maier, E. Sajovic, W. Lindner, *J. Chromatogr. A* **2004,** *1053*, 119–131.
7. H. Brunner, J. Bügler, B. Nuber, *Tetrahedron: Asymmetry* **1995**, *6*, 1699–1702.
8. E. Grochowski, J. Jurczak, *Synthesis* **1977**, *4*, 277–279.
9. S. Capasso, L. Mazzarella, A. J. Kirby, S. Salvadori, *Biopolymers* **1997**, *40*, 543–551.
10. C. Carlini, A. Fissi, G. Raspolli, A. M. Galletti, G. Sbrana, *Macromol. Chem. Phys.* **2000**, *201*, 1540–1551.
11. P. Dydio, C. Rubay, T. Gadzikwa, M. Lutz, Martin; J. N. H. Reek, *J. Am. Chem. Soc.* **2011**, *133*, 17176–17179.
12. K. M. Engle, D. H. Wang, and J. Q. Yu, *J. Am. Chem. Soc.*, **2010**, *132*, 14137–14151
13. T. Fornstedt, P. Sajonz, G. Guiochon, *J. Am. Chem. Soc.* **1997**, *119*, 1254–1264; T. Fornstedt, G. Guiochon, *Anal. Chem.* **2001**, *73*, 608A–617A; V. Schurig, *J. Chromatogr. A* **2009**, *1216*, 1723–1736.
14. J. Lah, N. M. Maier, W. Lindner, G. Vesnaver, *J. Phys. Chem. B* **2001**, *105,* 1670–1678; b) P. Levkin, N.M. Maier, W. Lindner, V. Schurig, submitted to JCA.
15. H. Brunner, P. Schmidt, M. Prommesberger, *Tetrahedron: Asymmetry* **2000**, *11*, 1501–1512; U. Sundermeier, C. Döbler, G. M. Mehltretter, W. Baumann, M. Beller, Chirality **2003**, *2*, 127–134.

Povzetek

Trije novi kiralni selektoji kinkonskega tipa so bili pripravljeni z vezavo *N*-pivaloilglicinskega, *N*-pivaloil-*(S)*-alaninskega in *N*-pivaloil-*(R)*-valinskega segmenta na *C9*-aminsko skupino 9-amino-9-(deoksi)-epikinina (eAQN). Imobilizirani so bili na silikagel in tako tvorili kiralne stacionarne faze (CSP). Vrednotenje kromatografskih enantioseparacijskih sposobnosti CPS za širok nabor N-karbamoilnih aminokislin vsebovanih v polarnih mobilnih fazah kaže na sposobnost kiralnega prepoznavanja za derivate *N*-Fmoc-, *N*-Cbz- in *N*-Boc. Ugotovili smo, da je enantioselektivno vezanje aminokislin na dane CSP natančno regulirano z absolutno streokemijo aminokislinskih skupin pripetih na *C9*-aminsko skupino ogrodja eAQN. V tej luči CPS izpeljana iz selektorja na osnovi *(S)*-valina kaže preferenčno vezavo *N*-karbamoil-*(S)*-aminokislin, CPS izpeljani iz selektorjev na osnovi *(R)*-valina in glicina pa nasprotno enantioselektivno preferenco vezanja. Opažen vpliv strukture analiziranih aminokislin na enantioselektivnost in specifične preference v enantioselektivnem vezanju kažejo na mehanizem kiralnega prepoznavanja, ki je osnovan na tvorbi ionskih parov in vodikovih vezi ter za prepoznavanje ključnih steričnih interakcijah. Ugotovitev, da je značilnosti kiralnega prepoznavanja epikinina mogoče dobro kontrolirati z vključitvijo skupin z dodatnimi stereogenimi centri na kinkonski skelet, lahko predstavlja koristno informacijo pri načrtovanju novih enantioselektivnih receptorjev in organokatalizatorjev.